度が高いとされ，かなり簡便であるが，蛍光強度のquentingで検出する方法のため，HPLC測定法に比較すると正確性に欠ける恐れがある。

4．細胞内での鉄代謝と細胞内不安定鉄

循環血液中に認められ得る不安定鉄としてNTBIがあげられたが，細胞内においても不安定な鉄は存在する。

血液中に存在する鉄は，ヘモグロビン合成やDNA合成をはじめとした各種の代謝に必須であるため全身の細胞に取り込まれるが，取り込まれた後の細胞内においても鉄は厳密に制御される必要がある。各種代謝に利用されず，細胞にとって余分となった鉄は，主に細胞質内のフェリチンと呼ばれる蛋白に格納される。フェリチンは，H-subunitとL-subunitという異なる2種類の分子が合計24個集合して構成されており，卵の殻のような形状で，内部に最大で4,500分子の鉄を貯蔵することができる[22]。このフェリチンのおかげで，細胞内では多くの鉄はfreeの形では存在しないですみ，過剰鉄が細胞に毒性を示すことが防がれている。しかし，細胞内の一部の鉄はLIPと呼ばれるfreeな形で存在すると考えられている。LIPは，細胞内各小器官と細胞質内での鉄の受け渡しなどを，種々の不安定な形態で速やかに行っていると考えられている鉄の「プール」である。フェリチンは十分な鉄貯蔵能力を有している上，細胞内鉄濃度が上昇すると，細胞はフェリチン蛋白の合成を亢進させてさらに格納能力を増やすように機能している。しかしながら，これらを超えるほど細胞内に多量の鉄が流入してくるようになると，フェリチンに格納しきれない分がLIPの増加につながる。LIPはfreeの鉄であるため容易にROS産生に働き，細胞障害をもたらすことになる。

LIPの存在形態に関しては詳細は不明な部分も多いが，Fe^{2+}とFe^{3+}両方の鉄イオン形態で存在し，鉄との親和性がそれほど強くない低分子物質と結合している。そのような低分子のキレート物質としては，アデニンやグアニンのような核酸，システインやチロシンのようなアミノ酸，あるいはクエン酸，アスコルビン酸，リン酸，リン脂質，ポリペプチドといった低分子化合物などが知られている。LIPは細胞内鉄総量の3～5%程度とその割合は極めて少ないとされるが，理論的には細胞内に取り込まれた鉄は，必ず一度はLIPを通過して目的となる鉄結合蛋白に至ることとなる。

LIPの動態には細胞内の種々の小器官が関与しており[23]，平衡状態でのLIPレベルは，細胞内への鉄の供給，細胞内における鉄の需要，細胞外への排出のバランスによって調整されている。組織によってその様式は大きく異なるものの，細胞外から細胞内への鉄の取り込みに関しては，例えばTfR1を介したTf結合鉄の取り込み経路や，Fe^{2+}のトランスポーターであるdivalent metal transporter 1（DMT1）[24, 25]やZIP14[26]などを介したNTBIの取り込み経路が知られている（図4）。TfR1を介した鉄取り込みであっても，細胞内エンドソーム内ではTfからはずれたFe^{3+}がFe^{2+}に還元された後，エンドソーム上のDMT1によって細胞内に移動するため，いずれの経路によっても，細胞質に移動した直後の鉄はFe^{2+}と考えられている。細胞にTf結合鉄やNTBIを負荷することにより細胞内のLIPレベルが増加することが知られており，細胞内への鉄供給がLIPレベルを規定する因子であると言えるが，これに加えて，細胞内からのLIPへの鉄供給も認められる。例えばフェリチンは，鉄を貯蔵し有害な鉄を隔離する機

DMT1 (divalent metal transporter 1)

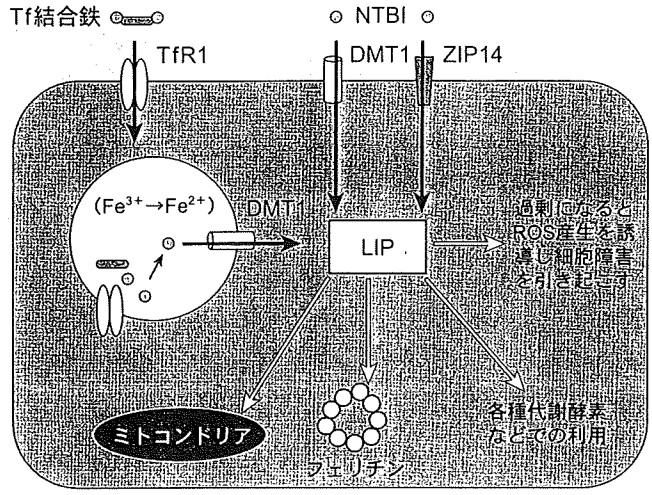

図4　細胞内のLIP

細胞は，トランスフェリン結合鉄(Tf結合鉄)をトランスフェリン受容体1（transferrin receptor 1：TfR1)で取り込んだり，NTBIをDMT1やZIP14などのtransporterによって取り込む。これらはいずれにしても一度細胞質内においてLIPとなり，それからミトコンドリアで利用されたり，フェリチンに格納されたり，その他の各種代謝に利用されたりする。細胞内でのバランスが崩れLIPが過剰になると，細胞に対して障害をもたらす。

能を有しLIPレベルを減少させる蛋白であるが，逆にLIPレベルが減少した際には蓄えた鉄分子を放出しそのレベルを維持している。また，主たる赤血球の処理細胞である網内系細胞においては，ヘム蛋白がheme oxygenase-1により分解されて生じる鉄は，LIP形成に重要な因子となる。

LIPレベルは臓器の種類によって異なっている[27]。例えば，赤血球産生を行う赤芽球では，Tfからの鉄はミトコンドリアのferrochelataseに非常に効率的に渡されヘム合成に使用されるため，細胞質にはほとんどLIPは検出できないと報告されている[28]。一方，マクロファージなどの網内系細胞では，赤血球を貪食しヘモグロビンを分解し，heme oxygenase-1によるヘム鉄の放出が行われているため，LIPの増加が予測されている。また，鉄の貯蔵を主に担う肝細胞においてもLIPの存在が確認されている[11]。

各細胞内小器官におけるLIPレベルも，細胞の種類によって異なると考えられている。ミトコンドリアは細胞内の主要な鉄消費器官であるが，同時にスーパーオキシドの産生部位でもある。ミトコンドリアでは，ヘムや鉄-硫黄クラスター蛋白へ取り込まれる鉄と，ミトコンドリアに入る鉄量は厳密にリンクしていることから，ミトコンドリア内のLIPレベルは非常に少ないと考えられている。しかし，キレート可能な鉄の存在が培養肝細胞や心筋細胞のミトコンドリア内に認められ，キレート物質がミトコンドリア内でのROS産生を抑制することも報告されている[29]。また，鉄-硫黄クラスター蛋白合成に必須のfrataxin蛋白異常に起因するFriedreich's ataxiaや，ミトコンドリアの鉄トランスポーターであるABC7遺伝子の異常であるX連鎖性鉄芽球性貧血などのようなミトコンドリア内に鉄蓄積を来す疾患においては，ミトコンドリア内のLIPが増加し，病態形成に寄与している可能性も考えられている[30]。

5．鉄キレート療法

これまで見てきたように，循環血液中のNTBIや細胞内におけるLIPは，フリーの形で存在する「不安定鉄」であり，細胞障害を引き起こし，各種の臓器障害にも強く関連していることが明らかとなってきた。こうした「不安定鉄」に対する治療として，単純ではあるがそれらの不安定鉄を除去する方法がまず考えられ，鉄キレート剤を用いた鉄キレート療法が期待される（表1）。

わが国では鉄過剰症に対して使用可能な唯一の

表1　鉄キレート剤の比較

	Desferrioxamine	Deferiprone	Deferasirox
投与経路	静注，皮下注	経口	経口
血漿中半減期	短い（5～20分程度）	やや短い（< 2 hours）	長い（8～16 hours）
投与方法	反復投与や持続投与が望ましい	1日2～3回の分割投与	1日1回投与
Molar chelating efficiency	High (hexadentate)	Low (bidentate)	Moderate (tridentate)
副作用	聴覚障害，骨や成長への影響，注射部位への局所皮膚反応など	重篤な顆粒球減少など	消化器症状，軽度の発疹，軽度の血清クレアチニン上昇（腎障害）など

現在まで臨床応用されている3つの鉄キレート剤の比較を示す。

治療薬がDFOであった。DFOの登場はサラセミア・メジャー患者の生存率を向上させたが，血中半減期は約5～20分と短く，経口バイオアベイラビリティが低いのが欠点で，静脈内または皮下投与が行われるが，さらに十分な血中濃度を保つために反復投与や持続ポンプを使用しての皮下注射などの工夫が必要であった。そのため，コンプライアンスも当然のことながら不良であり，十分な臨床効果をあげられる症例は多くなかった。

欧州で使用されているdeferiproneは低分子量で2座配位の経口鉄キレート剤であり，心臓に蓄積した鉄を効果的に除去するとされるが，血中半減期が約1.5時間程度と短いため1日2～3回の分割投与が必要であり，さらに顆粒球減少症の副作用が出やすいという問題があった。

一方，最近本邦でも認可になったdeferasiroxは新規トリデント鉄キレート剤であり，鉄に高い選択性を示す3座キレート剤である。血中半減期が8～16時間と長いため，1日1回水に懸濁して服用することで，定期的なDFO投与と同等の有効性が認められる。有害事象も他剤にくらべ少なく，コンプライアンスを高めることができ，鉄過剰症の予防および治療に非常に期待が持たれている。Deferasiroxの投与で，サラセミアの患者においてLPIが実際に低下するという報告もある。さらに，deferasiroxは細胞内に入ることから細胞内LIPもキレートする可能性が考えられ，鉄キレート療法が生体内不安定鉄を取り除くことで，将来的に鉄過剰によってもたらされ得る臓器障害を軽減，もしくは回避する可能性が示唆されている。

文　献

1) Aisen P, Enns C, Wessling-Resnick M: Chemistry and biology of eukaryotic metabolism. Int J Biochem Cell Biol **33**: 940-959, 2001
2) Gomme PT, McCann KB, Bertolini J: Transferrin: structure, function and potential therapeutic actions. Drug Discov Today **10**: 267-273, 2005
3) Andrews NC: Forging a field: the golden age of iron biology. Blood **112**: 219-230, 2008
4) Halliwell B, Gutteridge JMC: Role of free radicals and catalytic metal ions in human disease: an overview. Methods Enzymol **186**: 1-85, 1990
5) Ohhira M, Ohtake T, Matsumoto A, et al: Immunohistochemical detection of 4-hydroxy-2 nonenal-modified-protein adducts in human alcoholic liver diseases. Alcohol Cin Exp Res **22**: 145S-149S, 1998
6) Kato J, Kobune M, Nakamura T, et al: Normalization of elevated hepatic 8-hydroxy-2'-deoxyguanosine levels in chronic hepatitis C patients by phlebotomy and low iron diet. Cancer Res **61**: 8697-8702, 2001
7) Sahlstedt L, von Bonsdorff L, Ebeling F, et al: Effective binding of free iron by a single intra-

venous dose of human apotransferrin in haematological stem cell transplant patients. Br J Haematol 119 : 547-553, 2002
8) Breuer W, Hershko C, Cabantchik ZI : The importance of non-transferrin bound iron in disorders of iron metabolism. Transfus Sci 23 : 185-192, 2000
9) Greenberg GR and Wintrobe MW : A labile iron pool. J Biol Chem 165 : 397-398, 1946
10) Jacobs A : An intracellular transit iron pool. Ciba Found Symp 51 : 91-106, 1976
11) Kakhlon O, Cabantchik ZI : The labile iron pool : characterization, measurement, and participation in cellular processes (1) . Free Radic Biol Med 33 : 1037-1046, 2002
12) Scheiber-Mojdehkar B, Lutzky B, Schaufler R, et al : Non-transferrin-bound iron in the serum of hemodialysis patients who receive ferric saccharate : no correlation to peroxide generation. J Am Soc Nephrol 15 : 1648-1655, 2004
13) De Feo TM, Fargion S, Duca L, et al : Non-transferrin-bound iron in alcohol abusers. Alcohol Clin Exp Res 25 : 1494-1499, 2001
14) Bradley SJ, Gosriwitana I, Srichairatanakool S, et al : Non-transferrin-bound iron induced by myeloablative chemotherapy. Br J Haematol 99 : 337-343, 1997
15) Pepper JR, Mumby S, Gutteridge JM : Blood cardioplegia increases plasma iron overload and thiol levels during cardiopulmonary bypass. Ann Thorac Surg 60 : 1735-1740, 1995
16) Aisen P : Transferrin receptor 1. Int J Biochem Cell Biol 36 : 2137-2143, 2004
17) Hershko C, Graham G, Bates GW, Rachmilewitz EA : Non-specific serum iron in thalassaemia : an abnormal serum iron fraction of potential toxicity. Br J Haematol 40 : 255-263, 1978
18) Cabantchik ZI, Breuer W, Zanninelli G, Cianciulli P : LPI-labile plasma iron in iron overload. Best Pract Res Clin Haematol 18 : 277-287, 2005
19) Singh S, Hider RC, Porter JB : A direct method for quantification of non-transferrin-bound iron. Anal Biochem 186 : 320-323, 1990
20) von Bonsdorff L, Lindeberg E, Sahlstedt L, Lehto J, Parkkinen J : Bleomycin-detectable iron assay for non-transferrin-bound iron in hematologic malignancies. Clin Chem 48 : 307-314, 2002
21) Esposito BP, Breuer W, Sirankapracha P, et al : Labile plasma iron in iron overload : redox activity and susceptibility to chelation. Blood 102 : 2670-2677, 2003
22) Harrison PM, Arosio P : The ferritins : molecular properties, iron storage function and cellular regulation. Biochim Biophys Acta 1275 : 161-203, 1996
23) Breuer W, Shvartsman M, Cabantchik ZI : Intracellular labile iron. Int J Biochem Cell Biol 40 : 350-354, 2008
24) Gunshin H, Mackenzie B, Berger UV, et al : Cloning and characterization of a mammalian proton-coupled metal-ion transporter. Nature 388 : 482-488, 1997
25) Shindo M, Torimoto Y, Saito H, et al : Functional role of DMT1 in transferrin-independent iron uptake by human hepatocyte and hepatocellular carcinoma cell, HLF. Hepatol Res 35 : 152-162, 2006
26) Liuzzi JP, Aydemir F, Nam H, Knutson MD, Cousins RJ : Zip14 (Slc39a14) mediates non-transferrin-bound iron uptake into cells. Proc Natl Acad Sci U S A 103 : 13612-13617, 2006
27) Kruszewski M : Labile iron pool : the main determinant of cellular response to oxidative stress. Mutat Res 531 : 81-92, 2003
28) Richardson DR, Ponka P, Vyoral D : Distribution of iron in reticulocytes after inhibition of heme synthesis with succinylacetone : examination of the intermediates involved in iron metabolism. Blood 87 : 3477-3488, 1996
29) Glickstein H, El RB, Shvartsman M, Cabantchik ZI : Intracellular labile iron pools as direct targets of iron chelators : a fluorescence study of chelator action in living cells. Blood 106 : 3242-3250, 2005
30) Napier I, Ponka P, Richardson DR : Iron trafficking in the mitochondrion : novel pathways revealed by disease. Blood 105 : 1867-1874, 2005

doi:10.1016/j.jmb.2010.01.026 J. Mol. Biol. (2010) xx, xxx–xxx

JMB

Available online at www.sciencedirect.com
ScienceDirect

ELSEVIER

Characterization of the Interaction between Diferric Transferrin and Transferrin Receptor 2 by Functional Assays and Atomic Force Microscopy

Katsuya Ikuta[1,2]*, Alexandre Yersin[3], Atsushi Ikai[2,3], Philip Aisen[2] and Yutaka Kohgo[1]

[1]*Division of Gastroenterology and Hematology/Oncology, Department of Medicine, Asahikawa Medical College, 2-1-1-1 Midorigaoka-Higashi, Asahikawa, Hokkaido 078-8510, Japan*

[2]*Department of Physiology and Biophysics, Albert Einstein College of Medicine, 1300 Morris Park Avenue, Bronx, NY 10461, USA*

[3]*Graduate School of Bioscience and Biotechnology, Tokyo Institute of Technology, 4259-B8 Nagatsuta-cho, Midori-ku, Yokohama 226-8501, Japan*

Received 11 August 2009; received in revised form 29 December 2009; accepted 13 January 2010

Edited by W. Baumeister

Transferrin receptor 2 (TfR2), a homologue of the classical transferrin receptor 1 (TfR1), is found in two isoforms, α and β. Like TfR1, TfR2α is a type II membrane protein, but the β form lacks transmembrane portions and therefore is likely to be an intracellular protein. To investigate the functional properties of TfR2α, we expressed the protein with FLAG tagging in transferrin-receptor-deficient Chinese hamster ovary cells. The association constant for the binding of diferric transferrin (Tf) to TfR2α is $5.6 \times 10^6\ M^{-1}$, which is about 50 times lower than that for the binding of Tf to TfR1, with correspondingly reduced rates of iron uptake. Evidence for Tf internalization and recycling via TfR2α without degradation, as in the TfR1 pathway, was also found. The interaction of TfR2α with Tf was further investigated using atomic force microscopy, a powerful tool used for investigating the interaction between a ligand and its receptor at the single-molecule level on the living cell surface. Dynamic force microscopy reveals a difference in the interactions of Tf with TfR2α and TfR1, with Tf–TfR1 unbinding characterized by two energy barriers, while only one is present for Tf–TfR2. We speculate that this difference may reflect Tf binding to TfR2α by a single lobe, whereas two lobes of Tf participate in binding to TfR1. The difference in the binding properties of Tf to TfR1 and TfR2α may help account for the different physiological roles of the two receptors.

Keywords: iron metabolism; transferrin; transferrin receptor 2; atomic force microscopy; functional assay

Introduction

Iron is essential for all living organisms and is required for numerous metabolic processes. In vertebrates, and at least in some invertebrates with circulatory systems, almost all circulating iron is carried by diferric transferrin (Tf) to provide iron for cellular needs. The initial event in the cellular uptake of iron is the binding of Tf to transferrin receptor 1 (TfR1)[1] on the plasma membrane of cells, followed by endocytosis of the Tf–TfR1 complex. HFE[2]—the protein that, when mutated, is responsible for hereditary hemochromatosis—has been shown to combine with TfR1

*Corresponding author. 2-1-1-1 Midorigaoka-Higashi, Asahikawa, Hokkaido 078-8510, Japan. E-mail address: ikuta@asahikawa-med.ac.jp.

Present address: A. Yersin, Gymnase de Beaulieu, Rue du Maupas 50, 1004 Lausanne, Switzerland.

Present address: A. Ikai, Innovation Laboratory, Tokyo Institute of Technology (S2-8), 4259, Nagatsuta-Cho, Midori-Ku, Osaka, Japan.

Abbreviations used: TfR2, transferrin receptor 2; TfR1, transferrin receptor 1; Tf, diferric transferrin; AFM, atomic force microscopy; CHO, Chinese hamster ovary; PBS, phosphate-buffered saline; TCA, trichloroacetic acid; PTA, phosphotungstic acid; GFP, green fluorescent protein; BSA, bovine serum albumin.

0022-2836/$ - see front matter © 2010 Published by Elsevier Ltd.

Please cite this article as: Katsuya Ikuta, et al., Characterization of the Interaction between Diferric Transferrin and Transferrin Receptor 2 by Functional Assays and Atomic Force Microscopy, *J. Mol. Biol.* (2010), doi:10.1016/j.jmb.2010.01.026

Q1

and to reduce its affinity for Tf,[3–6] but the physiological functions of HFE are still not fully understood. In the acidified Tf-bearing endosome, iron is released from Tf and carried into the cytosol by divalent metal transporter 1.[7–9] After the release of its iron, Tf, still bound to the receptor in the acidified endosome, is recycled to the cell membrane and released from TfR1 at the cell surface where iron-free Tf is not bound by the receptor at pH 7.4. Most cells other than hepatocytes have been thought to depend chiefly or exclusively on the TfR1 cycle for securing iron from Tf.[10–12]

A second transferrin receptor, transferrin receptor 2 (TfR2), was cloned and identified as a new member of the transferrin receptor class.[13] TfR2 has two isoforms: TfR2α and TfR2β. TfR2α is thought to be a type II membrane protein like classical TfR1.[14] TfR2β is probably an intracellular protein because its amino acid sequence lacks transmembrane portions. Although its affinity for Tf is less than that for TfR1, TfR2α binds Tf and therefore may participate in cellular iron uptake, while the physiological function of TfR2β is unknown. Mutations of the TfR2 gene reduce hepcidin expression, resulting in iron overload and indicating that TfR2 may function primarily as a regulator of hepcidin production. However, the precise mechanisms of TfR2α involvement in cellular iron metabolism have not been elucidated, largely due to lack of information about the properties of the TfR2α protein. We therefore aimed to characterize the interactions of TfR2α with Tf by functional assays and atomic force microscopy (AFM), a powerful tool for investigating the interaction between a ligand and its receptor at the single-molecule level on a living cell surface.[15]

Results

Total protein contents

TfR1-deficient Chinese hamster ovary (CHO) TRVb cells were transfected with a TfR2α expression vector or mock vector, with no detectable change in cell morphology observed in culture wells by light microscopy. The total protein contents were 113± 20 pg/cell ($n=10$) for wild-type TRVb cells, 127± 19 pg/cell ($n=10$) for TRVb-TfR2α cells, and 120± 15 pg/cell ($n=10$) for TRVb mock cells. Thus, transfection of TRVb cells with the TfR2α expression vector did not cause any remarkable change in cellular protein concentration.

Expression of TfR2α and its binding to Tf

Transfection of TRVb cells with the TfR2α expression vector resulted in much higher Tf binding at 4 °C compared to wild-type TRVb cells or the mock-transfected clone (Fig. 1). Tf binding to TRVb cells and TRVb mock cells showed a nonsaturable, almost linear, behavior characteristic of nonspecific binding. In contrast, expressed cell surface Tf binding sites in TRVb-TfR2α cells saturated at 2.8×10^4 Tf molecules/cell, with the association constant K_a calculated to be 5.6×10^6 M^{-1}. Since TRVb-TfR2α cells and TRVb mock cells were maintained at 30 μg/ml puromycin, but TRVb cells were maintained without puromycin, TRVb mock cells were used as controls for further studies.

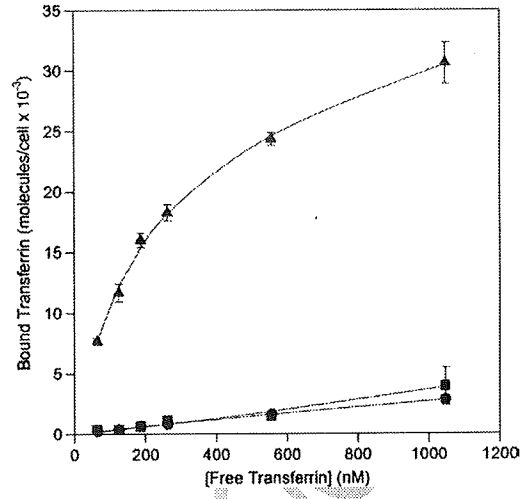

Fig. 1. Tf binding to TRVb (●), TRVb-TfR2α (▲), and TRVb mock cells (■) at 4 °C. Cells were incubated with [^{125}I]Tf at 4 °C for 1 h, washed to remove unbound Tf, and then solubilized for counting. TRVb-TfR2α cells showed a saturable binding curve, with an association constant of 5.6×10^6 M^{-1} and 2.8×10^4 binding sites/cell. The experiment was performed in triplicate.

Cell-associated Tf at 37 °C

Total cell-associated Tf at 37 °C increased as a function of Tf concentration in TRVb-TfR2α cells (Supplementary Fig. 1). The cell-associated Tf of TRVb mock cells, however, also increased as a function of Tf concentration, even though cell-associated Tf was less than that seen in TRVb-TfR2α cells. To determine whether transfection was responsible for this increase in cell-associated Tf in mock cells, we measured cell-associated Tf in wild-type TRVb cells at 37 °C. There was no remarkable difference between wild-type TRVb and TRVb mock cells, indicating that transfection itself did not cause the Tf association in mock cells (data not shown). Since TRVb cells lack detectable TfR1, this association with Tf must be receptor-independent. The difference between cell-associated Tf in TRVb-TfR2α cells and cell-associated Tf in TRVb mock cells as a function of Tf concentration—presumably due to Tf bound to TfR2α and Tf internalized via TfR2α in the former, but not in the latter—approached a constant value.

Please cite this article as: Katsuya Ikuta, et al., Characterization of the Interaction between Diferric Transferrin and Transferrin Receptor 2 by Functional Assays and Atomic Force Microscopy, *J. Mol. Biol.* (2010), doi:10.1016/j.jmb.2010.01.026

Q1

t1.2 **Table 1.** Tf internalized by TRVb-TfR2α cells via TfR2α

t1.3	Procedure	Molecules/cell
t1.4	[1] Total Tf associated with TRVb-TfR2α cells after incubation for 1 h at 37 °C	47,800
t1.5	[2] Cell-associated Tf after acid washing	26,500
t1.6	[3] Tf removed by acid washing	21,300
t1.7	[4] Tf initially bound to TfR2α at the cell surface (10/9 × [3])	23,700
t1.8	[5] Tf initially bound to TfR2α at the cell surface but resistant to acid washing	2370
t1.9	[6] Tf internalized by all pathways ([2]–[5]), also non-specifically bound and resistant to acid washing	24,100
t1.10	[7] Tf in mock cells (non-specifically bound and resistant to acid wash)	6600
t1.11	[8] Tf internalized via TfR2α in TRVb-TfR2α cells ([6] and [7])	17,500

Efficiency of the acid wash method

Our acid wash method removed approximately 90% of the cell surface membrane-bound Tf in TRVb-TfR2α cells compared to normal phosphate-buffered saline (PBS) washing (data not shown). In addition to acid washing, washing with F-12 medium was necessary to remove bound Tf, suggesting that, like TfR1, TfR2α binds apotransferrin at acidic pH but not at neutral pH.[14] Addition of cold Tf into F-12 medium at pH 7.4 did not enhance the effectiveness of washing, verifying that washing at pH 7.4 is sufficient for removing cell-surface-bound apotransferrin.

Evidence for Tf internalization mediated by TfR2α

After 1 h of incubation at 37 °C, cell-associated Tf in TRVb-TfR2α cells and TRVb mock cells represents both internalized Tf and nonspecific cell-surface-bound Tf that are resistant to acid washing. Tf in TRVb-TfR2α cells was 26,500 molecules/cell, much higher than the 6600 molecules/cell seen in TRVb mock cells (Table 1). Although the effectiveness of the acid wash method is only about 90%, the difference in cell-associated Tf between transfected cells and mock cells is too great to be attributed to residual cell-surface-bound Tf and therefore represents Tf internalized via TfR2α. We calculate that about 17,500 Tf molecules/cell are internalized by TfR2α (Table 1).

Iron uptake

Iron uptake by TRVb-TfR2α cells after 1 h of incubation at 37 °C was not clearly different from that by TRVb mock cells, even though there were small differences at high concentrations of Tf (Fig. 2a). To investigate whether or not induced TfR2α protein actually can donate iron to the cells, we determined the time course of ^{59}Fe uptake. Only after 1 h did a difference between TRVb-TfR2α cells and TRVb mock cells become clear (Fig. 2b). Thus, TfR2α-associated Tf could donate iron to cells, although its rate of donation is much less than that provided by Tf associated with TfR1. The data also indicate that CHO cells exhibit receptor-independent iron uptake from Tf, as described earlier.[16]

Efflux of Tf

To investigate the fate of Tf taken up through TfR2α, we incubated TRVb-TfR2α cells with ^{125}I-labeled Tf and acid-washed them before the time course of efflux was determined (Fig. 3). At time 0, Tf internalization by TRVb-TfR2α cells was higher than

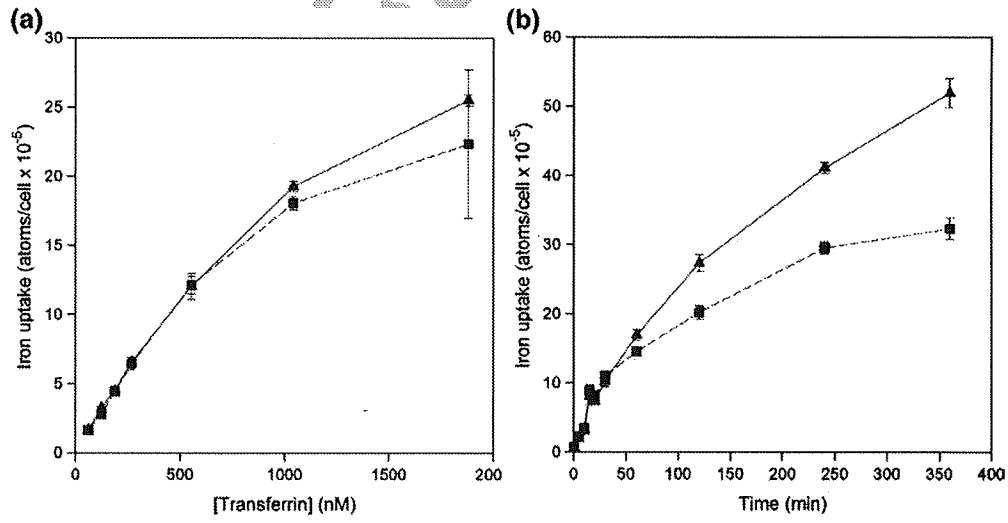

Fig. 2. Iron uptake at 37 °C as a function of Tf concentration (a). TRVb-TfR2α cells (▲) and TRVb mock cells (■) were incubated with [^{59}Fe]Tf at 37 °C for 1 h, washed to remove unbound Tf, and then solubilized for counting. This experiment was performed in triplicate. Iron uptake at 37 °C with time was also investigated (b). TRVb-TfR2α cells (▲) and TRVb mock cells (■) were incubated with 8.1×10^{-7} M [^{59}Fe]Tf at 37 °C for the indicated time, washed to remove unbound Tf, and then solubilized for counting. This experiment was also performed in triplicate.

Please cite this article as: Katsuya Ikuta, et al., Characterization of the Interaction between Diferric Transferrin and Transferrin Receptor 2 by Functional Assays and Atomic Force Microscopy, *J. Mol. Biol.* (2010), doi:10.1016/j.jmb.2010.01.026

Q1

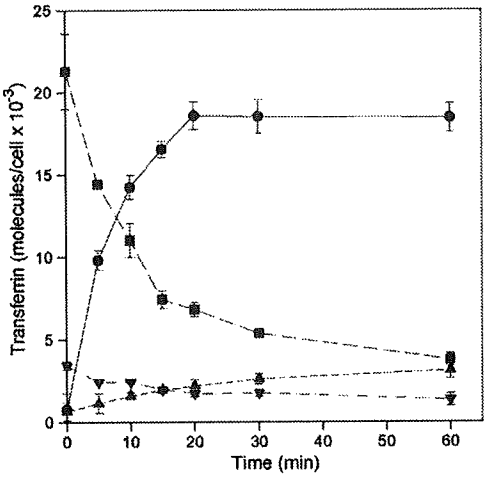

Fig. 3. Time course of Tf efflux. TRVb-TfR2α cells and TRVb mock cells were incubated with 3.5×10^{-7} M [^{125}I]Tf at 37 °C for 1 h, washed to remove unbound Tf, and then acid-washed to remove Tf bound to cell surface receptors. Cells were then incubated at 37 °C for the indicated times, the medium was collected, and solubilized cells were taken for counting. Tf exocytosed into the medium from TRVb-TfR2α cells (●) and TRVb mock cells (▲), and Tf retained in TRVb-TfR2α cells (■) and TRVb mock cells (▼), are shown. Experiments were performed in triplicate.

Tf internalization by TRVb mock cells, in keeping with Tf internalization by TfR2α, as discussed above. Internalized Tf mediated by TfR2α was exocytosed from TRVb-TfR2α cells; approximately 80% of Tf taken up via TfR2α was released by 30 min. The indication is that an effective efflux route exists for Tf taken up by TfR2α, suggesting that TfR2α, like TfR1, is recycled by the cells.

In a further investigation of the TfR2α pathway, the degradation of Tf internalized by TfR2α was determined. After 60 min, approximately 90% of Tf exocytosed from TRVb-TfR2α cells was precipitable by trichloroacetic acid (TCA)/phosphotungstic acid (PTA), indicating that Tf bound to TfR2α has recycled without substantial degradation in cells.

Pulse-chase study

To determine the fraction of cell-membrane-bound Tf that is internalized and the recycling time, we performed a pulse-chase experiment (Supplementary Fig. 2). Almost all Tf initially bound to TfR2α at 4 °C was released into the culture medium after 10 min of incubation at 37 °C, and there was no significant internalization of cell-surface-bound Tf in the single cycle of this pulse-chase study.

Absence of TfR1–TfR2 heterodimers

The effectiveness of anti-FLAG M2 antibody and anti-TfR1 antibody in immunoprecipitation had been confirmed before these experiments were undertaken (data not shown). HuH-7 cells, which express detectable TfR1 by Western blot analysis, were transiently transfected with the TfR2α expression vector, and cell lysates were taken for immunoprecipitation and Western blot analysis (Supplementary Fig. 3). Western blot analysis by anti-TfR1 antibody for the samples without immunoprecipitation showed that HuH-7 cells and HuH-7 cells transfected with TfR2α express almost identical amounts of TfR1. Furthermore, Western blot analysis by anti-TfR2 antibody for the samples not subjected to immunoprecipitation showed that HuH-7 cells transfected with TfR2α express more TfR2α proteins than nontransfected HuH-7 cells. These data indicated that the transiently transfected cells overexpressed TfR2α protein and that the antibodies were highly effective for Western blot analysis. When immunoprecipitation was performed with anti-TfR1 antibody, a band was clearly detected in transfected and nontransfected cells, but no band was found with the anti-TfR2 antibody. If a TfR1–TfR2 heterodimer were present, anti-TfR1 antibody would precipitate that protein, and Western blot analysis with anti-TfR2 antibody would show the band. When immunoprecipitation was performed with anti-FLAG M2 antibody, a 100-kDa band was detected only in transfected cells when the anti-TfR2 antibody was used as the primary antibody in Western blot analysis, indicating that transient transfection resulted in expression of immunoprecipitable TfR2α protein. No band was detected when anti-TfR1 was used as the primary antibody. Prolonged exposure of the blotted membrane to the developing solution did not make a difference. The possibility that the N-terminal FLAG tag in TfR2α interferes with dimer formation is unlikely, since the recombinant TfR1 lacking the first 120 N-terminal intracellular residues spontaneously dimerizes.[17] These results indicate that no detectable heterodimer of TfR1 and TfR2α was formed by the TfR2α-transfected HuH-7 cells. Therefore, our experiments detect TfR2, not the heterodimer of TfR1 and TfR2.

Specificity of detection by AFM

HLF cells (human hepatoma) were transiently cotransfected with TfR2α and green fluorescent protein (GFP) for identification, and tested with a Tf-coated tip. Retraction force curves were recorded with a Tf-coated tip and showed specific unbinding events between Tf on the tip and TfR2α at the cell surface (in Tris-buffered saline, pH 7.4) (Fig. 4a). The probability of binding between the Tf-coated tip and the TfR2 at the cell surface reached 26% ($n=7$ cells). In contrast, when nontransfected cells were tested with a Tf-coated tip, this probability was only 6% ($n=12$ cells, $p<0.001$, t test). This indicated that transient transfection of the TfR2α expression vector was adequate for the investigation using AFM (Fig. 4b).

Please cite this article as: Katsuya Ikuta, et al., Characterization of the Interaction between Diferric Transferrin and Transferrin Receptor 2 by Functional Assays and Atomic Force Microscopy, *J. Mol. Biol.* (2010), doi:10.1016/j.jmb.2010.01.026

Q1

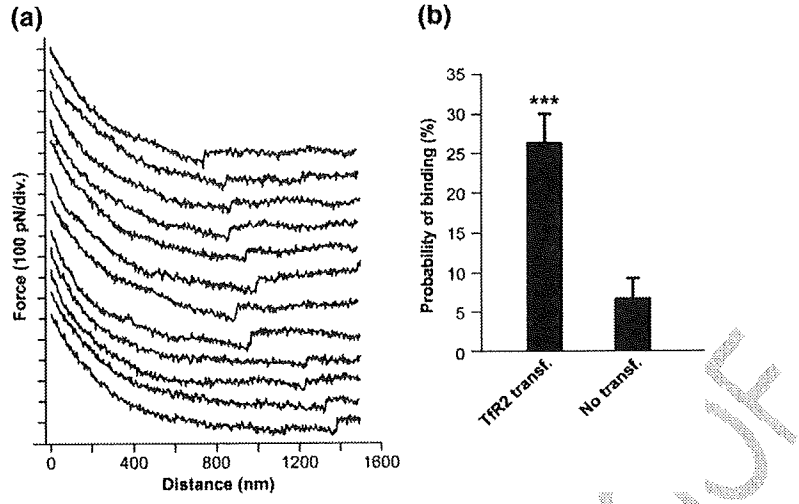

Fig. 4. (a) Retraction force curves on living HLF cells, transfected with TfR2α. The curves show specific unbinding events between Tf on the probe tip and TfR2α at the cell surface [in Tris-buffered saline (pH 7.4)]. (b) Specificity of detection by AFM. HLF cells (human hepatoma) were transiently cotransfected with TfR2α and GFP, and tested with a Tf-coated tip. The probability of binding was 26% ($n=7$ cells). In contrast, on nontransfected cells, the probability was only 6% ($n=12$ cells, $p<0.001$,***t test).

Force histogram for specific interaction between Tf and TfR2α

We recorded 1500 force curves with a Tf-coated tip on TfR2-transfected cells, allowing us to collect a total of 573 specific unbinding events in an experiment performed with a single tip using two cells. Events were analyzed and plotted in a force histogram (Fig. 5). A clear peak was visible on the histogram, showing that the mean unbinding force between Tf on the tip and TfR2 at the cell surface was 63±8 pN (at a mean loading rate of 2.8 nN/s). The experiment was repeated several days later using a new tip with cells independently cultured and gave similar results.

Dynamic force spectroscopy

Dynamic force spectroscopy, which consists of measuring the mean unbinding force at different loading rates, was performed with a Tf-coated tip on TfR2-transfected cells. As expected, the force was logarithmically dependent on the loading rate (Fig. 6). However, this dependence was small, as the force varied from 59±9 pN at a rate of 1.7 nN/s to 62±10 pN at a rate of 20 nN/s. In striking contrast, the unbinding force between TfR1 and Tf was reported at 39±5 pN at a rate of 1 nN/s and

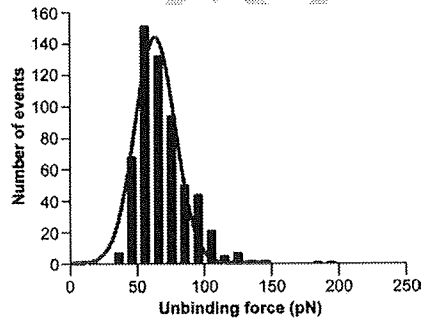

Fig. 5. Force histogram for the specific interaction between Tf and TfR2α on HLF cells. The histogram was obtained from an analysis of 573 unbinding events collected over 1500 force curves. The mean unbinding force is 63±8 pN for a mean loading rate of 2.8 nN/s. The gray line represents a Gaussian fit.

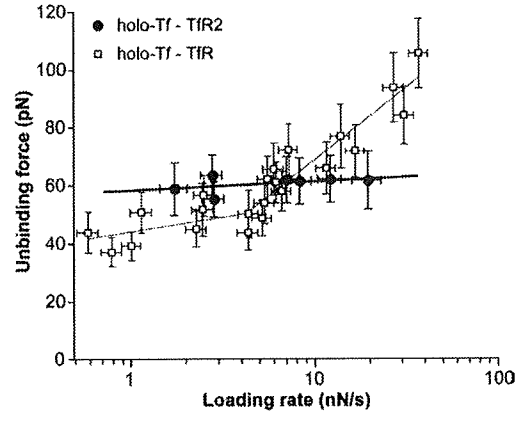

Fig. 6. Dynamic force spectroscopy of Tf–TfR2α (black dots). The unbinding force is plotted as a function of the loading rate logarithm. For comparison, the force spectrum of Tf–TfR1 is also shown. Only one regime is evident for TfR2, but two can be seen for TfR1, clearly revealing the different interactions of the two proteins with Tf.

Please cite this article as: Katsuya Ikuta, et al., Characterization of the Interaction between Diferric Transferrin and Transferrin Receptor 2 by Functional Assays and Atomic Force Microscopy, *J. Mol. Biol.* (2010), doi:10.1016/j.jmb.2010.01.026

Q1

increased up to 94±12 pN at a rate of 27 nN/s,[15] indicating that the binding of TfR2α and Tf differs from the binding of TfR1 and Tf. Furthermore, the force spectrum of TfR2-transfected cells displayed only one regime (slope), while two regimes were clearly visible for TfR1-expressing cells (Fig. 6), implying different interactions of Tf with TfR1 and TfR2.

Discussion

In their original publication, Kawabata *et al.* reported that TfR2α can bind Tf and donate iron to CHO cells,[13] therefore supporting cell growth.[14] Fleming *et al.* found that TfR2 expression is not regulated by intracellular iron status and thus might be involved in the pathogenesis of hemochromatosis.[18] Although TfR2 is thus shown to function in iron metabolism, its precise physiological role is still unknown.

To avoid confusion by TfR1, our first studies used HuH-7 cells with anti-sense suppressed TfR1 expression.[19,20] The amount of residual TfR1, however, was still high, so that it was not possible to differentiate between Tf binding to TfR1 and Tf binding to TfR2α because of the low affinity of TfR2α for Tf.[14] We therefore turned to TfR1-deficient CHO cells for expressing TfR2α.[13,21]

In the present study, the affinity of TfR2α for Tf was measured in living cells for the first time using [^{125}I]Tf to display the binding isotherm at 4 °C. The K_a for the binding of Tf by TfR2α was calculated to be 5.6×10^6 M^{-1}, about 35-fold less than that for the binding of Tf by TfR1 (2×10^8 M^{-1} to 3×10^8 M^{-1} in HuH-7 cells). The lower affinity of TfR2α in transfected CHO cells is in accordance with a previous report based on a qualitative study by flow cytometry.[14] Quantification by surface plasmon resonance using a recombinant soluble extracellular portion of the receptor gave a binding constant of 37×10^6 M^{-1}, consistent with the present result, considering the difference in methodology.[22] The deduced amino acid sequence of the extracellular domain of TfR2α protein is 45% identical and 66% similar to that of TfR1. TfR2α also possesses the RGD triad (amino acids 678–680),[13] which is thought to be critical for binding Tf to TfR1.[23] The lower affinity of TfR2α for Tf is now, therefore, not explicable.

Although the affinity of TfR2α for Tf is much less than that of TfR1, the concentration of iron-bearing Tf in the circulation (about 3×10^{-5} M) is sufficient to saturate TfR2α. TfR2α expression has been found in cells with active roles in iron metabolism. Liver, the principal organ of iron storage, expresses a high level of TfR2α mRNA, as do human hepatoma-derived HepG2 cells[13] and HuH-7 cells (unpublished observation). K562 cells, of human myelogenous erythroleukemic origin, also express TfR2α mRNA.[13] Studies of iron uptake from Tf prior to the discovery of TfR2 did not discriminate between the roles of the two receptors. In future studies, therefore, both receptors require consideration.

Binding of Tf to TRVb-TfR2α and TRVb mock cells at 4 °C was only 25–50% inhibited by a 100-fold excess of unlabeled Tf, possibly because of large, essentially nonsaturable binding. We therefore resorted to the use of a binding isotherm with terms for specific (saturable) and nonspecific (nonsaturable) binding to estimate the binding constants for each type of binding.[24] Curve-fitted parameters for specific binding attributable to transfected TfR2α were as follows: K_a, 5.6×10^6 M^{-1}; total number of sites, 2.8×10^4 $cell^{-1}$. These contrast with binding constants near 10^8 M^{-1} and site numbers in the range of 2×10^5 $cell^{-1}$ to 5×10^5 $cell^{-1}$ for Tf binding in K562 cells when TfR1 predominates and curve-fitting to a single class of sites adequately accounts for binding. An apparent binding constant of 6.5×10^9 M^{-1} is obtained for the nonsaturable binding of Tf to TRVb-TfR2α cells, substantially weaker than that derived for specific binding. At Tf concentrations of 10^{-6} M, for example, saturable binding would account for about 24,000 Tf molecules/cell, while nonsaturable binding would account for 6500 molecules/cell. Nevertheless, both TfR2α-dependent binding and nonspecific binding contribute to the association of Tf with the cells.

In the present study, CHO cells showed a receptor-independent association with Tf that should be considered when investigating the function of TfR2α expressed in CHO cells. We find a clear increase in cell-associated Tf after TfR2α expression. Since cell-associated Tf represents both cell-surface-bound Tf and Tf internalized via TfR2α, a proof of Tf internalization mediated by TfR2α was required. Cell-associated Tf persisting after acid washing confirmed the existence of Tf internalization via TfR2α.

After internalization, an efflux of Tf, without substantial degradation, is found. Thus, Tf internalized by TfR2α, like Tf internalized by TfR1, recycles. An important difference between the two receptors was observed in a pulse-chase study. Less than 12% of Tf bound to the cell surface of TRVb-TfR2α cells is internalized, with most of the Tf dissociated and released to the medium at 37 °C. In contrast, approximately 30–50% of membrane-bound Tf was internalized by human-hepatoblastoma-derived HepG2 cells[12] and human-hepatoma-derived HLF cells.[25] The lower affinity of TfR2α for Tf may help account for the difference between previous studies and the present work, since HepG2 and HLF cells express TfR1, but TRVb-TfR2α cells do not. In our pulse-chase study, no detectable internalization of membrane-bound Tf in a single cycle was found when the occupancy of TfR2α by transferrin was about 75%. In normal circulation, however, the concentration of iron-bearing Tf is close to 3×10^{-5} M, so that cell surface receptors are always saturated with Tf and replenished as Tf is internalized. TfR2α might therefore normally function in iron uptake from Tf, but this has yet to be experimentally confirmed.

Please cite this article as: Katsuya Ikuta, et al., Characterization of the Interaction between Diferric Transferrin and Transferrin Receptor 2 by Functional Assays and Atomic Force Microscopy, *J. Mol. Biol.* (2010), doi:10.1016/j.jmb.2010.01.026.

Overexpressed TfR2α protein was also shown to mediate iron uptake, although its rate of iron donation was slow. We estimate, from the difference between iron uptake by TRVb-TfR2α cells and iron uptake by TRVb mock cells in Fig. 2b, that the rate of iron uptake was approximately 0.2 atom/receptor/min when cells were incubated with 8.1×10^{-7} M Tf. For comparison, the rate of iron uptake via TfR1 was about 0.5–1 atom/receptor/min in K562 cells. Thus, TfR2α may function in iron uptake from Tf, albeit with less efficiency than TfR1.

Because of the sequence similarities between TfR1 and TfR2α, the possibility that the protein monomers combine to form heterodimers was investigated. However, no detectable expression of heterodimers was found in the present studies. The possibility that our transfection procedure in HuH-7 cells yielded two different cell populations (one expressing TfR2α and the other failing to do so) must be considered, so that expression of heterodimers was too low for detection. We cannot exclude the possibility of heterodimer formation that might be detected by more sensitive methods or in other cells.

AFM was used to characterize the interactions between Tf and TfR2α protein at the single-molecule level. We found that the unbinding force needed to detach Tf from TfR2α (63±8 pN) was different from the unbinding force needed to detach Tf from TfR1, previously reported as 56±7 pN.[15] However, dynamic force measurements revealed striking differences between Tf–TfR1 and Tf–TfR2α interactions, which reflected clearly distinct energy landscapes.[15] While Tf–TfR1 unbinding is characterized by two energy barriers, only one is present for Tf–TfR2. This obvious difference might arise from different binding points for Tf–TfR1 and Tf–TfR2α interactions. In addition, this possibility provides a structural interpretation for the energy barriers postulated here. We speculate that the two barriers of the Tf–TfR1 interaction stem from the binding of both lobes of Tf (C-lobe and N-lobe), whereas the single barrier of Tf–TfR2α interaction originates from the binding of a single lobe, but we recognize that this speculation requires further investigation.

In conclusion, the present study shows that TfR2α protein functions in binding Tf and taking up iron, and that there must be a difference between TfR1 and TfR2 in their interactions with Tf, as revealed by AFM. TfR2α mRNA lacks an IRE, so that expression is not regulated by intracellular iron status[18] but possibly by cell cycle.[14] Furthermore, TfR2 cannot compensate for TfR1 in TfR1 knockout mice, which lack a functional Tf cycle and do not survive gestation.[26] A nonsense mutation of the human TfR2 gene causes a hemochromatosis-like disorder.[27,28] The physiological functions of TfR2 are therefore still unclear, although it likely contributes to the regulation of cellular iron status.

Materials and Methods

Cells and cell culture

TfR1-deficient CHO TRVb cells[21] were grown in F-12 Nutrients Mixture (Invitrogen, Grand Island, NY) supplemented with 5% heat-inactivated fetal bovine serum (Gemini Bio-Products, Woodland, CA), 100 U/ml penicillin, and 100 μg/ml streptomycin. All cultures were maintained at 37 °C in 5% CO_2.

TfR2α expression vector

Total RNA was extracted from K562 cells using the RNAgent Total RNA Isolation System (Promega, Madison, WI) following the manufacturer's instructions. Complementary DNA was reverse-transcribed from 1 μg of RNA using an oligo-dT primer (Promega) and MMLV reverse transcriptase (Stratagene, La Jolla, CA), and human TfR2α cDNA was amplified by hot-start PCR. A FLAG sequence was added to the 5′-terminus of the cDNA to enable detection of expressed protein by anti-FLAG antibodies. The oligonucleotides used as PCR primers were 5′-ACCTTAAGGCCACCATGGATTACAAGGATGACGACGATAAGATGGAGCGGCTTTG-3′ and 5′-GGTTCGAAGCAATGAGAGGTGGAC-3′. The conditions for amplification were as follows: 40 cycles of 99 °C for 1 min, 65 °C for 2 min, and 72 °C for 5 min. The amplified DNA fragment was digested with AflII and BstBI, and then inserted into the bicistronic mammalian expression vector pIRESpuro2 (Clontech, Palo Alto, CA). The orientation and sequence of the inserted TfR2α cDNA fragment were confirmed by sequencing.

Transfection

TRVb cells were grown in 35-mm six-well plates until they had reached 70–80% confluence, then they were transfected with the TfR2α expression vector using Lipofectamine Plus (Invitrogen, Carlsbad, CA). Selection was performed with 10 μg/ml puromycin (Clontech) for 2 weeks, and then the concentration of the antibiotic was raised to 30 μg/ml in order to isolate a clone with high-level expression of TfR2α. After another 2 weeks, one viable colony (TRVb-TfR2α) was obtained and then subcultured using a cloning cylinder. As mock-transfected controls, TRVb cells were transfected with the pIRESpuro2 vector without a cDNA insert, and one clone was isolated after 4 weeks of selection (TRVb mock cells). These transfectants were maintained at 30 μg/ml puromycin after isolation. Expression of TfR2α mRNA was confirmed by reverse transcriptase PCR, and the expression of TfR2α protein was confirmed by immunoprecipitation–Western blot analysis using anti-FLAG antibodies (data not shown).

Total protein content

The total protein contents of TRVb, TRVb-TfR2α, and TRVb mock cells were determined with the Bio-Rad Protein Assay Kit (Bio-Rad, Hercules, CA) using bovine serum albumin (BSA) as standard. Cells were counted with a hemocytometer.

Please cite this article as: Katsuya Ikuta, et al., Characterization of the Interaction between Diferric Transferrin and Transferrin Receptor 2 by Functional Assays and Atomic Force Microscopy, *J. Mol. Biol.* (2010), doi:10.1016/j.jmb.2010.01.026

Q1

Iodination of Tf

Human Tf (Boehringer-Mannheim, Germany) was labeled with ^{125}I (Amersham Pharmacia Biotech, Piscataway, NJ) by the iodine monochloride method of McFarlane.[29] To remove unbound ^{125}I, we passed labeled Tf through a 10-DG desalting column (Bio-Rad) two times. Specific activities were observed in the range of 100–200 cpm/ng Tf, and more than 95% of ^{125}I was protein-bound as determined by precipitation with 20% TCA/4% PTA.

^{59}Fe labeling of Tf

Iron was removed from Tf, and labeling with ^{59}Fe was carried out by previously described methods.[30] Specific activities were in the range of 2000–3500 cpm/ng Fe. In some experiments, apotransferrin was labeled with ^{125}I, as described above, and then loaded with ^{59}Fe.

Binding assay

Tf binding assays were performed as previously reported.[31] Cell numbers were calculated from protein concentrations determined with the Bio-Rad Protein Assay Kit. Each experiment was performed in triplicate. The total number of specific binding sites per cell and the K_a for the binding of Tf to these sites were estimated from nonlinear least-squares curve fitting to a saturable binding isotherm:[32]

$$\text{occupied sites} = \frac{\text{total sites} \times K_a[\text{Tf}]}{1 + K_a[Tf]},$$

from which it is also possible to calculate the fraction of sites occupied by Tf at any concentration of free Tf.

Tf and iron uptake

Cells were plated at a density of 1×10^6 cells/well in 35-mm six-well plates 24 h before the experiments. Cells were preincubated with F-12 three times for 10 min at 37 °C, chilled on ice for 30 min, and then incubated at 37 °C with F-12 containing 2% BSA and labeled Tf at indicated concentrations and times. Cells were then washed with ice-cold PBS five times and solubilized by 0.1% Triton X-100 for counting.

Acid washing of cells

To remove cell-surface-receptor-bound Tf, we washed cells with ice-cold PBS five times and then incubated them with ice-cold acid wash buffer [0.025 M citric acid, 0.025 M sodium citrate, 200 μM deferoxamine mesylate, and 0.15 M sucrose (pH 4.0)] for 3 min, followed by two 2-min incubations with ice-cold F-12 medium to remove cell-surface-bound apotransferrin. Finally, the cells were washed once more with ice-cold PBS. This method removed approximately 90% of surface-bound Tf in TRVb-TfR2α cells.

Efflux of Tf from cells

Cells, plated at a density of 1×10^6 cells/well in 35-mm six-well plates 24 h before the experiments, were preincubated with F-12 three times for 10 min at 37 °C, chilled on ice for 30 min, and then incubated with F-12 containing 2% BSA and 3.5×10^{-7} M ^{125}I-labeled Tf for 60 min at 37 °C. After acid washing, fresh F-12 medium was added, and cells were again incubated at 37 °C. At indicated times, F-12 media were collected, and cells were washed with ice-cold PBS and solubilized by 0.1% Triton X-100. Media and cell lysates were then taken for γ-counting. After counting, media were incubated with 10% TCA/2% PTA for 30 min on ice, and then centrifuged at 14,000 rpm in an Eppendorf centrifuge for 20 min. Tf degradations were calculated from the radioactivities of supernatants and precipitates.

Pulse-chase study

TRVb-TfR2α cells were incubated with 5.1×10^{-7} M [^{125}I]Tf, as previously described, for 1 h at 4 °C. Cells were then washed with ice-cold PBS five times. Fresh F-12 medium was added, and cells were incubated at 37 °C. At indicated times, cells were chilled on ice, and media were immediately collected. Cells were again washed with ice-cold PBS, and media were collected. Cells were then acid washed to quantify surface-bound Tf and solubilized for the measurement of intracellular Tf.

Immunoprecipitation–Western blot analysis

Human-hepatoma-derived HuH-7 cells were transiently transfected with the TfR2α expression vector, as described above. At 48 h after transfection, 5×10^6 cells were washed with PBS five times and collected with a cell scraper. Harvested cells were dissolved in 40 μl of the cell extraction buffer of the Mammalian Cell Extraction Kit (BioVision Incorporated, Mountain View, CA) following the manufacturer's instructions for Western blot analysis without immunoprecipitation, or in 1.5 ml of lysis buffer [10 mM Tris–HCl, 150 mM NaCl, 1% Nonidet P-40, 1 mM ethylenediaminetetraacetic acid, and 1 mM PMSF containing 1:2000 Protease Inhibitor Cocktail (Boehringer-Mannheim; pH 7.4)] for immunoprecipitation–Western blot analysis. Freezing and thawing were performed three times, following which samples were centrifuged at 2700*g*. Protein G Sepharose (Amersham Biosciences, Uppsala, Sweden) was added, and preparations were incubated at 4 °C for 8 h, then centrifuged at 1500*g* for 5 min. Supernatants were then collected for incubation with anti-FLAG M2 antibody (Sigma), which recognizes FLAG at any location in the target protein, or with anti-TfR1 antibody (Zymed Laboratory, South San Francisco, CA) for 8 h at 4 °C. Protein G Sepharose was added, and incubation continued for an additional 8 h at 4 °C. Samples were centrifuged at 1500*g* for 5 min, and pellets were washed with PBS five times. Concentrated dye buffer was added, and final concentrations were adjusted to 10 mM Tris–HCl, 1 mM ethylenediaminetetraacetic acid, 2.5% SDS, 5% β-mercaptoethanol, and 0.01% bromophenol blue (pH 8.0). Samples were then immersed in boiling water for 5 min and centrifuged at 20,000*g* for 5 min to remove precipitated material. Electrophoresis using a 12% gradient polyacrylamide gel and transfer to a nitrocellulose membrane were carried out. The transfer membrane was incubated with anti-TfR2 antibody (9F8 1C11) (Santa Cruz Biotechnology, Inc., Santa Cruz, CA) diluted 1:200 or with anti-TfR1 antibody diluted 1:1000, and then with horseradish-peroxidase-conjugated goat anti-mouse IgG antibody (R&D Systems, Minneapolis,

Please cite this article as: Katsuya Ikuta, et al., Characterization of the Interaction between Diferric Transferrin and Transferrin Receptor 2 by Functional Assays and Atomic Force Microscopy, *J. Mol. Biol.* (2010), doi:10.1016/j.jmb.2010.01.026

MN) diluted 1:2000. SuperSignal West Pico Chemiluminescent Substrate (Thermo Scientific, Rockford, IL) was used as development substrate.

Atomic force microscopy

The details of the methods for investigation using AFM were previously reported.[15] In brief, the probe of AFM is a sharp tip placed at the end of a soft cantilever. A piezoelectric scanner allows the precise positioning of the tip relative to the sample. A laser beam reflected on the cantilever backside and detected by photodiodes is used to measure cantilever deflection. This signal is either used as feedback to control the scanner (imaging mode) or measured and converted into force (force spectroscopy mode). Since the cantilever is mounted under the scanner, the optical path is free, and AFM can be coupled to an optical microscope. Tf was linked to the AFM tip by a three-step functionalizing protocol. First, SiN tips are aminosilanized by exposure to APTES vapors. Second, a heterobifunctional polyethylene glycol linker is anchored to amino-group-bearing tips through its NHS end. Third, Tf is attached to the polyethylene glycol linker free end via a maleimide–cysteine bond.

Measuring the interaction force between Tf and TfR2α by AFM

HLF cells (human hepatoma) were cotransfected with TfR2α and GFP for identification, as previously described.[33] A Tf-coated tip was brought in contact with the cell surface, allowing the proteins to bind. The tip was then retracted, resulting first in protein stretching, then unbinding. Cantilever deflections during one cycle are recorded in a force curve. A binding–unbinding event between Tf and TfR2α is represented by a sawtooth pattern on the curve. It allows calculation of the force necessary to unbind the two proteins, using the cantilever spring constant (Hooke's law). The mean unbinding force is obtained by fitting a Gaussian curve to the force histogram. The error on the mean unbinding force is calculated by adding the standard deviation of the sample and the error resulting from the spring constant calibration (10%). Moreover, the unbinding force is related to the pulling rate by:

$$F^* = \frac{k_B T}{x} ln\left(\frac{x}{k_0 k_B T}\right) + \frac{k_B T}{x} ln(r_f)$$

where F^* is the most probable unbinding force, k_0 is the dissociation rate constant, r_f is the loading rate applied, x is the width of the energy barrier along the direction of the applied force, k_B is the Boltzmann constant, and T is temperature.

Acknowledgements

We are grateful to Dr. Timothy E. McGraw for providing the CHO TRVb cells used in this study. This work was supported, in part, by grants 1 PO1 DK55495 and 5 RO1 DK015056 from the National Institutes of Health, US Public Health Service, USA.

Supplementary Data

Supplementary data associated with this article can be found, in the online version, at doi:10.1016/j.jmb.2010.01.026

References

1. Kühn, L. C., McClelland, A. & Ruddle, F. H. (1984). Gene transfer, expression, and molecular cloning of the human transferrin receptor gene. *Cell*, **37**, 95–103.
2. Feder, J. N., Gnirke, A., Thomas, W., Tsuchihashi, Z., Ruddy, D. A., Basava, A. *et al.* (1996). A novel MHC class I-like gene is mutated in patients with hereditary haemochromatosis. *Nat. Genet.* **13**, 399–408.
3. Feder, J. N., Penny, D. M., Irrinki, A., Lee, V. K., Lebrón, J. A., Watson, N. *et al.* (1998). The hemochromatosis gene product complexes with the transferrin receptor and lowers its affinity for ligand binding. *Proc. Natl Acad. Sci. USA*, **95**, 1472–1477.
4. Lebrón, J. A., Bennett, M. J., Vaughn, D. E., Chirino, A. J., Snow, P. M., Mintier, G. A. *et al.* (1998). Crystal structure of the hemochromatosis protein HFE and characterization of its interaction with transferrin receptor. *Cell*, **93**, 111–123.
5. Waheed, A., Parkkila, S., Zhou, X. Y., Tomatsu, S., Tsuchihashi, Z., Feder, J. N. *et al.* (1997). Hereditary hemochromatosis: effects of C282Y and H63D mutations on association with β2-microglobulin, intracellular processing, and cell surface expression of the HFE protein in COS-7 cells. *Proc. Natl Acad. Sci. USA*, **94**, 12384–12389.
6. Roy, C. N., Penny, D. M., Feder, J. N. & Enns, C. A. (1999). The hereditary hemochromatosis protein, HFE, specifically regulates transferrin-mediated iron uptake in HeLa cells. *J. Biol. Chem.* **274**, 9022–9028.
7. Gunshin, H., Mackenzie, B., Berger, U. V., Gunshin, Y., Romero, M. F., Boron, W. F. *et al.* (1997). Cloning and characterization of a mammalian proton-coupled metal-ion transporter. *Nature*, **388**, 482–488.
8. Fleming, M. D., Romano, M. A., Su, M. A., Garrick, L. M., Garrick, M. D. & Andrews, N. C. (1998). Nramp2 is mutated in the anemic Belgrade (b) rat: evidence of a role for Nramp2 in endosomal iron transport. *Proc. Natl Acad. Sci. USA*, **95**, 1148–1153.
9. Gruenheid, S., Canonne-Hergaux, F., Gauthier, S., Hackam, D. J., Grinstein, S. & Gros, P. (1999). The iron transport protein NRAMP2 is an integral membrane glycoprotein that colocalizes with transferrin in recycling endosomes. *J. Exp. Med.* **189**, 831–841.
10. Klausner, R. D., Van Renswoude, J., Ashwell, G., Kempf, C., Schechter, A. N., Dean, A. & Bridges, K. R. (1983). Receptor-mediated endocytosis of transferrin in K562 cells. *J. Biol. Chem.* **258**, 4715–4724.
11. Dautry-Varsat, A., Ciechanover, A. & Lodish, H. F. (1983). pH and the recycling of transferrin during receptor-mediated endocytosis. *Proc. Natl Acad. Sci. USA*, **80**, 2258–2262.
12. Ciechanover, A., Schwartz, A. L., Dautry-Varsat, A. & Lodish, H. F. (1983). Kinetics of internalization and recycling of transferrin and the transferrin receptor in a human hepatoma cell line. Effect of lysosomotropic agents. *J. Biol. Chem.* **258**, 9681–9689.
13. Kawabata, H., Yang, S., Hirama, T., Vuong, P. T., Kawano, S., Gombart, A. F. & Koeffler, H. P. (1999). Molecular cloning of transferrin receptor 2. A new member of the transferrin receptor-like family. *J. Biol. Chem.* **274**, 20826–20832.

Please cite this article as: Katsuya Ikuta, et al., Characterization of the Interaction between Diferric Transferrin and Transferrin Receptor 2 by Functional Assays and Atomic Force Microscopy, *J. Mol. Biol.* (2010), doi:10.1016/j.jmb.2010.01.026

14. Kawabata, H., Germain, R. S., Vuong, P. T., Nakamaki, T., Said, J. W. & Koeffler, H. P. (2000). Transferrin receptor 2-alpha supports cell growth both in iron-chelated cultured cells and *in vivo*. *J. Biol. Chem.* **275**, 16618–16625.
15. Yersin, A., Osada, T. & Ikai, A. (2008). Exploring transferrin–receptor interactions at the single-molecule level. *Biophys. J.* **94**, 230–240.
16. Chan, R. Y. Y., Ponka, P. & Schulman, H. M. (1992). Transferrin-receptor-independent but iron-dependent proliferation of variant Chinese hamster ovary cells. *Exp. Cell Res.* **202**, 326–336.
17. Lawrence, C. M., Ray, S., Babyonyshev, M., Galluser, R., Borhani, D. W. & Harrison, S. C. (1999). Crystal structure of the ectodomain of human transferrin receptor. *Science*, **286**, 779–782.
18. Fleming, R. E., Migas, M. C., Holden, C. C., Waheed, A., Britton, R. S., Tomatsu, S. *et al.* (2000). Transferrin receptor 2: continued expression in mouse liver in the face of iron overload and in hereditary hemochromatosis. *Proc. Natl Acad. Sci. USA*, **97**, 2214–2219.
19. Trinder, D., Zak, O. & Aisen, P. (1996). Transferrin receptor-independent uptake of diferric transferrin by human hepatoma cells with antisense inhibition of receptor expression. *Hepatology*, **23**, 1512–1520.
20. Sasaki, K., Zak, O. & Aisen, P. (1993). Antisense suppression of transferrin receptor gene expression in a human hepatoma cell (HuH-7) line. *Am. J. Hematol.* **42**, 74–80.
21. McGraw, T. E., Greenfield, L. & Maxfield, F. R. (1987). Functional expression of the human transferrin receptor cDNA in Chinese hamster ovary cells deficient in endogenous transferrin receptor. *J. Cell Biol.* **105**, 207–214.
22. West, A. P., Jr., Bennett, M. J., Sellers, V. M., Andrews, N. C., Enns, C. A. & Bjorkman, P. J. (2000). Comparison of the interactions of transferrin receptor and transferrin receptor 2 with transferrin and the hereditary hemochromatosis protein HFE. *J. Biol. Chem.* **275**, 38135–38138.
23. Dubljevic, V., Sali, A. & Goding, J. W. (1999). A conserved RGD (Arg-Gly-Asp) motif in the transferrin receptor is required for binding to transferrin. *Biochem. J.* **341**, 11–14.
24. Osterloh, K. & Aisen, P. (1989). Pathways in the binding and uptake of ferritin by hepatocytes. *Bioclim. Biophys. Acta*, **1011**, 40–45.
25. Ikuta, K., Fujimoto, Y., Suzuki, Y., Tanaka, K., Saito, H., Ohhira, M. *et al.* (2000). Overexpression of hemochromatosis protein, HFE, alters transferrin recycling process in human hepatoma cells. *Biochim. Biophys. Acta*, **1496**, 221–231.
26. Levy, J. E., Jin, O., Fujiwara, Y., Kuo, F. & Andrews, N. C. (1999). Transferrin receptor is necessary for development of erythrocytes and the nervous system. *Nat. Genet.* **21**, 396–399.
27. Camaschella, C., Roetto, A., Cali, A., De Gobbi, M., Garozzo, G., Carella, M. *et al.* (2000). The gene TFR2 is mutated in a new type of haemochromatosis mapping to 7q22. *Nat. Genet.* **25**, 14–15.
28. Roetto, A., Totaro, A., Piperno, A., Piga, A., Longo, F., Garozzo, G. *et al.* (2001). New mutations inactivating transferrin receptor 2 in hemochromatosis type 3. *Blood*, **97**, 2555–2560.
29. McFarlane, A. S. (1963). *In vivo* behavior of I-fibrinogen. *J. Clin. Invest.* **42**, 346–361.
30. Young, S. P. & Aisen, P. (1980). The interaction of transferrin with isolated hepatocytes. *Biochim. Biophys. Acta*, **633**, 145–153.
31. Zak, O., Trinder, D. & Aisen, P. (1994). Primary receptor-recognition site of human transferrin is in the C-terminal lobe. *J. Biol. Chem.* **269**, 7110–7114.
32. Klotz, I. M. & Hunston, D. L. (1971). Properties of graphical representations of multiple classes of binding sites. *Biochemistry*, **10**, 3065–3069.
33. Yersin, A., Hirling, H., Kasas, S., Roduit, C., Kulangara, K., Dietler, G. *et al.* (2007). Elastic properties of the cell surface and trafficking of single AMPA receptors in living hippocampal neurons. *Biophys. J.* **92**, 4482–4489.

Please cite this article as: Katsuya Ikuta, et al., Characterization of the Interaction between Diferric Transferrin and Transferrin Receptor 2 by Functional Assays and Atomic Force Microscopy, *J. Mol. Biol.* (2010), doi:10.1016/j.jmb.2010.01.026

 DOI 10.1002/prca.200900112 *Proteomics Clin. Appl.* 2009, *3*, 1256–1264

RESEARCH ARTICLE

Heterogeneous expressions of hepcidin isoforms in hepatoma-derived cells detected using simultaneous LC-MS/MS

Takaaki Hosoki[1], Katsuya Ikuta[1], Yasushi Shimonaka[2], Yusuke Sasaki[2], Hideyuki Yasuno[2], Kazuya Sato[1], Takaaki Ohtake[1], Katsunori Sasaki[3], Yoshihiro Torimoto[4], Keiji Saito[2] and Yutaka Kohgo[1]

[1] Division of Gastroenterology and Hematology/Oncology, Department of Medicine, Asahikawa Medical College, Asahikawa, Japan
[2] Kamakura Research Labs, Chugai Pharmaceutical Co., Ltd., Kamakura, Japan
[3] Department of Gastrointestinal Immunology and Regenerative Medicine, Asahikawa Medical College, Asahikawa, Japan
[4] Oncology Center, Asahikawa Medical College Hospital, Asahikawa, Japan

Hepcidin, a key regulator of iron homeostasis, is known to have three isoforms: hepcidin-20, -22, and -25. Hepcidin-25 is thought to be the major isoform and the only one known to be involved in iron metabolism; the physiological roles of other isoforms are poorly understood. Because of its involvement in the pathophysiology of hereditary hemochromatosis and the anemia of chronic disease, the regulatory mechanisms of hepcidin expression have been extensively investigated, but most studies have been performed only at the transcriptional level. Difficulty in detecting hepcidin has impeded *in vitro* research. In the present study, we developed a novel method for simultaneous quantification of hepcidin-20, -22, and -25 in the media from hepatoma-derived cell lines. Using this method, we determined the expression patterns of hepcidin isoforms and the patterns of responses to various stimuli in human hepatoma-derived cultured cells. We found substantial differences among cell lines. In conclusion, a novel method for simultaneous quantification of hepcidin isoforms is presented. Heterogeneous expressions of hepcidin isoforms in human hepatoma-derived cells were revealed by this method. We believe our method will facilitate quantitative investigation of the role hepcidin plays in iron homeostasis.

Received: June 3, 2009
Revised: July 13, 2009
Accepted: July 17, 2009

Keywords:
Hepatocyte / Hepcidin antimicrobial peptide / Iron metabolism / LC-MS/MS

Correspondence: Dr. Katsuya Ikuta, Division of Gastroenterology and Hematology/Oncology, Department of Medicine, Asahikawa Medical College, 2-1-1-1 Midorigaoka-Higashi, Asahikawa, Hokkaido 078-8510, Japan
E-mail: ikuta@asahikawa-med.ac.jp
Fax: +81-166-68-2469

Abbreviations: **Ct**, threshold cycle; **DFO**, desferrioxamine; **EMEM**, Eagle's minimum essential medium; **FAC**, ferric ammonium citrate; **HAMP**, hepcidin antimicrobial peptide; **holo-Tf**, holo-transferrin; **IL-1β**, interleukin-1β; **IL-6**, interleukin-6; **LPS**, lipopolysaccharide; **QC**, quality control; **qRT-PCR**, quantitative RT-PCR; **SRM**, selected reaction monitoring

1 Introduction

Hepcidin is a small peptide mainly produced by the liver, and it is thought to be the key regulator in iron homeostasis [1, 2]. Hepcidin binds to ferroportin, the mammalian iron exporter expressed on the basolateral side of enterocytes and on the cell surface of macrophages, thereby causing the internalization and degradation of ferroportin [3]. Hepcidin thus inhibits iron uptake from the gastrointestinal tract and iron release from reticuloendothelial cells, so that iron balance of the body is negatively regulated by hepcidin [1, 2]. Increased

hepcidin expression therefore leads to iron deficiency while decreased hepcidin expression causes iron overload.

Hepcidin is involved in several diseases, such as hereditary hemochromatosis and the anemia of chronic disease. In hereditary hemochromatosis, various mutations occur in genes such as *HFE*, *hemojuvelin*, and *transferrin receptor 2*, leading to decreased hepcidin expression despite generalized iron overload [4–6]. In contrast, in anemia of chronic disease, inflammatory cytokines such as interleukin-6 (IL-6) [7, 8] and interleukin-1β (IL-1β) [9, 10] upregulate hepcidin expression and thus cause iron-deficiency anemia.

Recently, the regulation of hepcidin expression has been intensively studied to reveal pathophysiological mechanisms involved in diseases in which iron metabolism is altered. For instance, the cytokine IL-6 increases hepcidin synthesis utilizing signal transducers and activators of transcription-3 during inflammation such as caused by systemic infections [11]. The bone morphogenic proteins (BMPs) are members of the transforming growth factor β superfamily, and BMPs have been proposed to be involved in hemojuvelin-mediated regulation of hepcidin synthesis [12]. However, almost all research on the regulation of hepcidin expression has been restricted to studying changes in transcription of the *hepcidin antimicrobial peptide* (*HAMP*) gene utilizing RT-PCR under various conditions.

Hepcidin is produced mainly by hepatocytes expressing the *HAMP* gene located on chromosome 19. The transcript of this gene is believed to produce a prepropeptide of 84 amino acids, and then the peptide is digested by furin, the intercellular convertase, and finally the mature form of hepcidin appears in the peripheral blood [13]. However, there is little information about the ratios of serum prohepcidin to mature hepcidin, and the secreted fraction of hepcidin to hepcidin retained intracellularly. In addition, kidney cells have been shown to produce hepcidin independently of the liver [14]. Therefore, there is no proof that *HAMP* transcript levels of the liver reflect total body secretion of hepcidin-25. Consequently, it is desirable that hepcidin be determined from peptide levels in the serum, in addition to transcriptional levels of the liver and other organs.

Three isoforms of mature hepcidin are known. A 25-amino acid peptide (hepcidin-25) is thought to be the major isoform [15], but other forms of hepcidin such as hepcidin-20 and -22 have been detected in human urine [16]. Only hepcidin-25 has been shown to cause the internalization and degradation of ferroportin. However, the possibility arises that hepcidin-20 and -22 have different physiological roles in homeostasis and their expressions are regulated independently from hepcidin-25. It is therefore desirable that hepcidin-20, -22, and -25 be separately quantified.

The first method for measuring prohepcidin, using ELISA, was reported by Kulaksiz *et al.* [17]. That method has been applied for the analysis of hepcidin expression levels, but there is little information about how and whether hepatocytes secrete prohepcidin into the blood [17]. Several groups have developed antibodies to detect and measure hepcidin, but difficulties for differentiation of hepcidin-20, -22, and -25 [18] persist. MS-based modalities have been used in recent years for measuring hepcidin. For instance, SELDI-TOF-MS has been used for semi-quantification [19, 20], and LC-MS/MS has been employed for quantification of hepcidin [21, 22]. These methods are applicable to assaying clinical samples such as blood and urine. Most recently, Ganz *et al.* reported development of an ELISA system for quantification of human serum hepcidin that is expected to be a powerful tool for clinical samples [23].

Experiments *in vitro* would also be valuable for investigating the complex molecular mechanisms regulating hepcidin expression. Detection and quantification of hepcidin in cell culture media has been difficult, probably due to its low concentration.

We therefore aimed to develop a sensitive new method for measuring hepcidin that can simultaneously measure hepcidin-20, -22, and -25 secreted in culture media by hepatoma-derived cells. We now report such a method, improving the MS-based modality that we previously reported [22]. We also determined the characteristics of hepcidin expression of various hepatoma cell lines using the new method, which can be applied to analyzing differences among hepatoma cells of varying lineage.

2 Materials and methods

2.1 Hepcidin standards

Human hepcidin-25 was obtained from the Peptide Institute (Osaka, Japan). Hepcidin-20, -22, and [$^{13}C_{18}$, $^{15}N_3$]-hepcidin-25 were synthesized at the Peptide Institute.

2.2 Chemicals

BMP2 and holo-transferrin (holo-Tf) were purchased from R & D Systems; IL-6 was obtained from Wako Pure Chemical Industries, Osaka, Japan. FBS was purchased from Japan Bioserum; Eagle's minimum essential medium (EMEM), DMEM, RPMI-1640 medium, L-glutamine, and sodium bicarbonate were purchased from Sigma-Aldrich. Penicillin–streptomycin solution were bought from Invitrogen. IL-1β was purchased from Wako Pure Chemical Industries; desferrioxamine (DFO), ferric ammonium citrate (FAC), lipopolysaccharide (LPS), and cobalt chloride were obtained from Sigma-Aldrich. Decanoyl-RVKR-CMK (furin inhibitor I) was purchased from Calbiochem (Darmstadt, Germany). All other chemicals and solvents were of analytical reagent grade.

2.3 Cell cultures

Human hepatoma-derived cell lines used in this study were HepG2, HuH-1, HuH-2, HuH-4, HuH-6, HuH-7, WRL68, HB611, Hep3B, HLE, HLF, SK-HEP-1, and human primary

hepatocytes derived from normal liver (Applied Cell Biology Research Institute).

HuH-4, HB611, and HuH-6 cells were incubated with RPMI1640; HuH-7 cells were incubated with DMEM. Other cells were incubated with EMEM. Those medium were supplemented with 10% FBS, 100 U/mL penicillin, and 100 μg/mL streptomycin. All cells were cultured at 37°C in a humidied incubator with 5% CO_2. In some experiments, FBS-free UltraCulture medium (Lonza, MD, USA) supplemented with 2 mM L-glutamine was used. HepG2 cells could survive in this serum-free medium for more than 3 days.

Cells at the density of 1×10^6 cells/mL were grown in 6-well plates for 24 h to almost 80% conuency in 2 mL of culture medium. Medium in each well was replaced by 2 mL of culture medium containing various stimulants and then incubated for 48 h. All cell lines were maintained with 20 ng/mL IL-6 or 30 μM holo-Tf or no additives for control cells.

After 48 h, culture media were collected and analyzed for hepcidin-20, -22, and -25 concentrations as follows: 50 μL of 4% trichloroacetic acid solution containing 200 ng/mL [$^{13}C_{18}$, $^{15}N_3$]-hepcidin-25 as internal standard was added to an equal amount of each culture medium, mixed vigorously, and centrifuged. A 20-μL aliquot of the resulting supernatant was analyzed quantitatively by LC-MS/MS. Cells were lysed with 0.1% Triton X-100 for protein assay, or by Sepazol™ (Nacarai Tesque, Japan) for RT-PCR studies.

HepG2 cells were also treated with various reagents instead of IL-6 or holo-Tf, such as 200 pg/mL IL-1β, 100 μM DFO, 100 μM FAC, 1 μg/mL LPS, 50 μM $CoCl_2$, or 50 μM furin inhibitor I. After 48 h, culture media were collected for quantification of hepcidin isoforms, and cells were lysed for measuring protein concentrations.

Each treatment was performed in triplicate, and data presented as mean and SD.

2.4 LC/ESI-MS/MS analysis

LC/ESI-MS/MS was performed using an API4000QTRAP (Applied Biosystems, Foster City, CA, USA) equipped with a UPLC ACQUITY™ systems (Waters). The turboionspray was operated in the positive ion mode at 5500 V for the ion spray voltage. Analytical chromatography of human hepcidin-20, -22, and -25 was accomplished on a PLRP-S column (5 μm, 300 Å, 150 mm × 2.0 mm id; Polymer Laboratories, Shropshire, UK). Instrument control and data processing were with Analyst™ software version 1.4 (Applied Biosystems).

2.5 Quantitative analysis of human hepcidin-20, -22, and -25

Selected reaction monitoring (SRM) transitions were as follows: human hepcidin-20, *m/z* 548.85 → 119.80; human hepcidin-22, *m/z* 610.14 → 119.80; human hepcidin-25, *m/z* 558.80 → 120.07; [$^{13}C_{18}$, $^{15}N_3$]-human hepcidin-25, *m/z* 563.11 → 109.60. The declustering potential for human hepcidin-20, -22, -25, and [$^{13}C_{18}$, $^{15}N_3$]-human hepcidin-25 were 50, 50, 81, and 81 V, respectively. The turboionspray source was maintained at a temperature of 600°C. Collision energies for human hepcidin-20, -22, -25, and [$^{13}C_{18}$, $^{15}N_3$]-human hepcidin-25 were 52, 59, 73 and 75 V, respectively. The collisional activation dissociation gas was set at 4. Mobile phase A was 0.1% aqueous formic acid, and mobile phase B was 0.1% formic acid in ACN. Gradient conditions were as follows: B 20% (0 min, 0.3 mL/min) → 20% (2.01 min, 0.3 mL/min) → 25% (5.00 min, 0.3 mL/min) → 25% (10.00 min, 0.3 mL/min) → 90% (10.01 min, 0.3 mL/min) → 90% (12.00 min, 0.3 mL/min) → 20% (12.01 min, 0.3 mL/min) → 20% (14.00 min, 0.3 mL/min).

Analysis of hepcidin-25 in the BMP2-stimulated HepG2 culture medium was performed on the 6520 quadrupole-TOF/MS (Agilent Technologies).

2.6 RNA isolation and quantitative RT-PCR

Total RNA was isolated and quantitative RT-PCR (qRT-PCR) was performed in a reaction mix containing TaqMan Universal PCR Master Mix No AmpErase UNG (Applied Biosystems), specific human *HAMP* primers, and probe (pre-validated Taqman gene expression assay, Applied Biosystems), and 100 ng of cDNA. All reactions were multiplexed with the housekeeping gene 18S, provided as a pre-optimized control probe (Applied Biosystems) enabling data to be expressed as delta threshold cycle (ΔCt) values (where ΔCt = Ct of 18 s subtracted from Ct of gene of interest). Reactions were as follows: 50°C for 2 min, 95°C for 10 min; then 60 cycles of 95°C for 15 s and 60°C for 1 min. All measurements were performed in triplicate, and relative *HAMP* mRNA expression was expressed as fold expression over the average of *HAMP* mRNA expression corresponding to the HepG2 cells.

2.7 Cellular protein assay

Cell were lysed with 0.1% Triton-X and total protein concentrations were determined using the Bradford reagent (BioRad, Hercules, CA, USA), following the manufacturer's instructions.

3 Results

3.1 Establishment of quantitative measurement of hepcidin isoforms

To improve further the method for quantifying small peptides by LC-MS/MS, we developed a quantitative and simultaneous method for hepcidin-20, -22, and -25 in

biological fluids. Upon optimization of SRM conditions, the most intense precursor ions were selected in each mass spectrum to detect hepcidin isoforms. Product ions were selected to maximize sensitivity and selectivity. Using EMEM supplemented with 10% FBS as matrix, various concentrations of synthetic hepcidin isoforms were spiked, and analyzed by LC-MS/MS. Isoform peaks were not interfered with by a blank matrix, indicating the method has good selectivity.

Our method was validated by specificity, linearity, lower limit of quantification, intra-assay precision, and accuracy. Calibration curves were constructed over the range 2–1000 ng/mL in the above matrix. Five replicates of 2, 5, 50, 500, and 1000 ng/mL of each isoform quality control (QC) samples were prepared and analyzed by LC-MS/MS.

There was no interference peak at retention time of each isoform, confirming good specificity (Fig. 1A). Linearity of the calibration curves by weighted ($1/x^2$) linear regression was excellent (correlation coefficient: $r = 0.9974$ for hepcidin-20, $r = 0.9937$ for hepcidin-22, $r = 0.9950$ for hepcidin-25; Fig. 1B). Accuracies of the back-corrected concentrations were within 87.4–109% for hepcidin-20, 80.1–110% for hepcidin-22, and 80.5–109% for hepcidin-25. The lower limits of quantification for each hepcidin isoform was 2 ng/mL. Coefficients of variance in intra-assay QC samples were 1.2–8.6% for hepcidin-20, 3.1–5.7% for hepcidin-22, and 1.5–7.0% for hepcidin-25. Accuracies for QC samples were 99.7–122.1% for hepcidin-20, 102.6–132.5% for hepcidin-22, and 99.1–141.2% for hepcidin-25. These results indicate that the method is adequate for quantifying hepcidin isoforms in culture media.

3.2 Detection of hepcidin isoforms in HepG2 media

In the SRM chromatogram of HepG2 medium analyzed by LC-MS/MS, peaks corresponding to the retention time of synthetic hepcidin-22 and -25, but not hepcidin-20, were detected. Peaks corresponding to hepcidin-22 and -25 were also detected and up-regulated in 100 ng/mL BMP2 stimulated HepG2 medium (Fig. 2A). No peaks corresponding to hepcidin-20 were founded in the chromatogram of HepG2 media at any tested conditions.

We tried to identify the component of the corresponding peak for hepcidin-25 in HepG2 medium. For that purpose, BMP2 medium was prepared because it contained a relatively high concentration of putative hepcidin-25, (65.9 ng/mL). Synthetic hepcidin-25 and BMP2 medium were analyzed by quadrupole-TOF/MS. The major precursor ions of synthetic hepcidin-25 ranged from $m/z = 558.4$–559.0. At the same retention time, precursor ions from BMP2 medium showed a similar distribution (Fig. 2B). Mass spectra of product ions were also similar. Several major common product ions were observed (Fig. 2C). Overall, synthetic hepcidin-25 and HepG2-derived peak components are similar in retention time and mass spectra of the

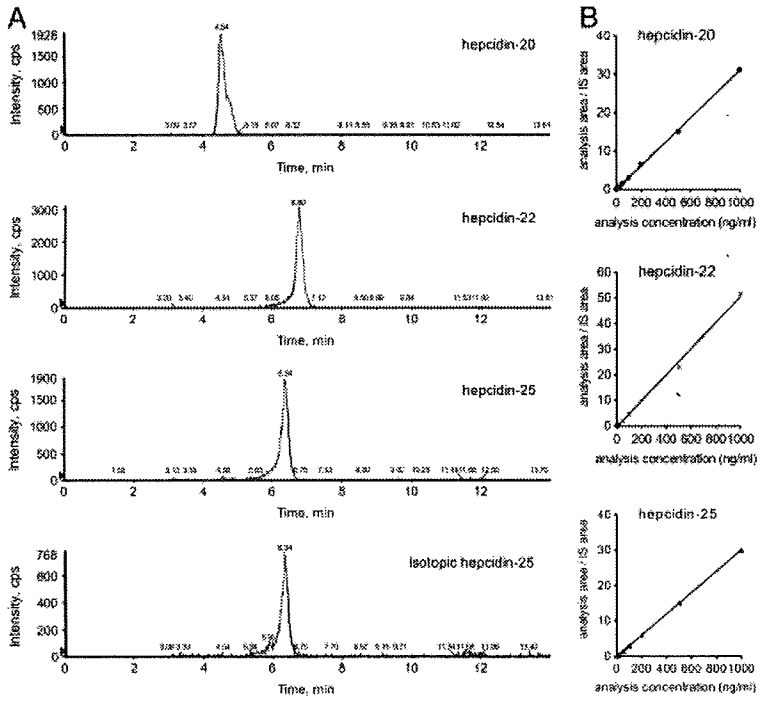

Figure 1. (A) Representative LC-MS/MS chromatograms of hepcidin-20, -22, -25, and blank isotopic hepcidin-25 sample. (B) The calibration curves of hepcidin-20, -22, and -25 in the culture medium are linear in the range of 2–1000 ng/mL. The correlation coefficients of calibration curves are as follows: hepcidin-20, $r = 0.9974$; hepcidin-22, $r = 0.9937$; hepcidin-25, $r = 0.9950$.

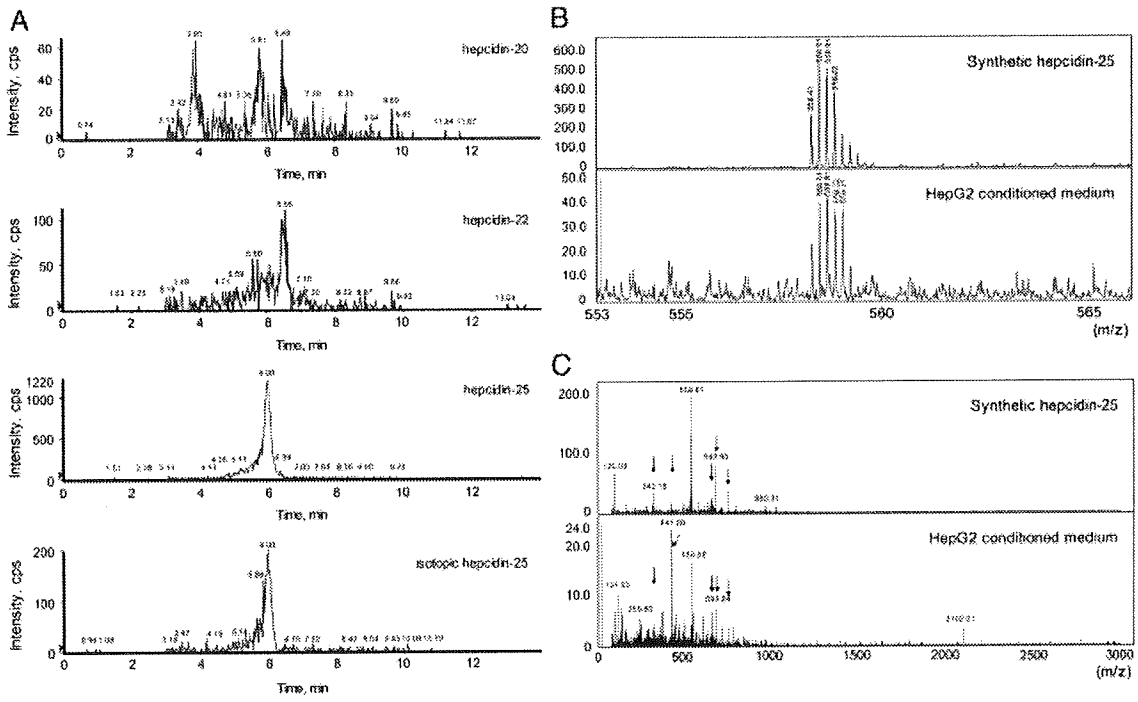

Figure 2. (A) Detection of hepcidin isoforms in BMP2-stimulated HepG2 medium. (B) MS spectra of synthetic hepcidin-25 and derived peak from BMP2-stimulated HepG2 medium showing similar patterns. (C) MS/MS spectra of synthetic hepcidin-25 and derived peak from BMP2-stimulated HepG2 medium showing similar patterns. Arrows show common fragments.

precursor ions and product ions, verifying that the peak detected in the culture medium represents hepcidin-25.

3.3 HAMP gene expressions in hepatoma-derived cell lines

We aimed at first to determine qualitatively whether cell lines derived from hepatocellular carcinomas express the *HAMP* gene as assayed by RT-PCR. Expression levels of *HAMP* mRNA differed among cell lines (Fig. 3A). HepG2, HuH-1, and HuH-7 cells showed relatively high *HAMP* mRNA expressions, but other cells exhibited only slight expressions. qRT-PCR was then performed (Fig. 3B). HepG2, HuH-1, and HuH-7 cells expressed high levels of *HAMP* mRNA, compatible with the results of qualitative RT-PCR. Only slight or moderate *HAMP* mRNA expression was found in other cells.

3.4 Quantification of hepcidin isoforms in the culture medium of various hepatoma-derived cell lines

HLE, HLF, SK-Hep1, and human primary hepatocytes did not show any detectable hepcidin isoforms in their culture media (data not shown). We could observe hepcidin isoforms in culture media from other cell lines. We also found that hepatoma-derived cell lines exhibited different patterns of hepcidin isoform expression and changes induced by various stimulations. Even among cell lines that secrete detectable hepcidin isoforms, four distinct patterns were discerned.

HepG2 cells expressed hepcidin-22 and -25, but not hepcidin-20. IL-6 significantly upregulated the expression of both isoforms, but holo-Tf suppressed hepcidin-25 expression (Fig. 4A).

WRL68 cells showed expression of hepcidin-20 and -22 even in control conditions, and holo-Tf stimulation increased both expressions significantly (Fig. 4B).

HuH-1 and HuH-7 cells expressed only hepcidin-25. IL-6 significantly increased the expression of hepcidin-25 in both cell lines. Addition of holo-Tf to the medium did not change the level of hepcidin-25 in HuH-1 cells, and even decreased hepcidin-25 in HuH-7 cells (Fig. 4C).

HB611, Hep3B, HuH-2, HuH-4, and HuH-6 showed expression of only hepcidin-20, but when holo-Tf was added, hepcidin-22 appeared (Fig. 4D).

We observed that some cell lines respond to holo-Tf by increasing the secretion of hepcidin-20 or -22. Although Lin *et al.* have reported *HAMP* mRNA expressions to be increased in mouse primary hepatocytes stimulated with

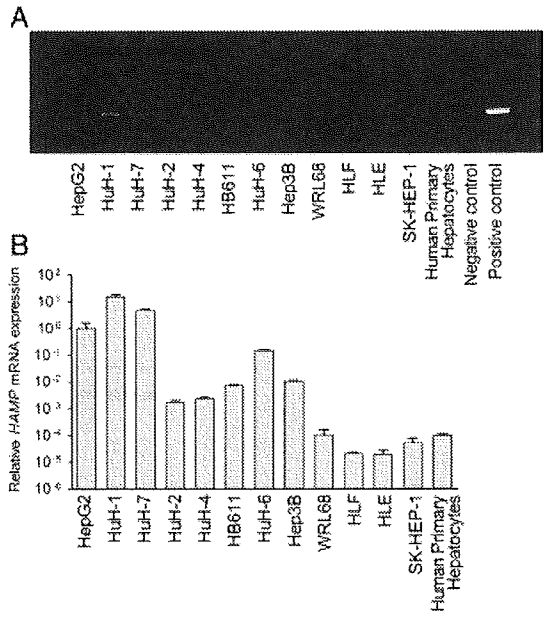

Figure 3. Expressions of *HAMP* mRNA in hepatoma-derived cell lines determined by qRT-PCR. (A) Qualitative RT-PCR showed that the expressions of *HAMP* mRNA were quite different among hepatoma-derived cell lines. (B) The expression levels of *HAMP* mRNA were standardized by 18*S* rRNA. Relative *HAMP* mRNA expression levels are shown as fold expression over the average of *HAMP* mRNA of HepG2 cells. HepG2, HuH-7, and HuH-1 cells highly express *HAMP* mRNA, while other cell lines exhibits only slight or moderate *HAMP* mRNA expressions.

human holo-Tf [24],] we believe ours is the first study showing upregulation of hepcidin at the peptide level by human holo-Tf in human cells. The physiological function of this effect is, however, not apparent since only hepcidin-25 is known to be involved in iron metabolism.

3.5 Determination of the changes of hepcidin expression in responses to various stimulations of HepG2 cells

The HepG2 cell line is one of the most frequently used hepatoma-derived lines for research and secretes mainly hepcidin-25, the only isoform reported to interact with ferroportin, into the culture medium.

Hepcidin expression has been reported to be regulated by inflammatory cytokines such as IL-6 and IL-1β; hence, HepG2 cells were stimulated with these cytokines. As shown in Fig. 5A, IL-6 significantly upregulates hepcidin-25, in agreement with earlier reports. A slight increase of hepcidin-22 was observed with IL-1β stimulation, but no obvious upregulation was seen in hepcidin-25. Iron overload has been reported to upregulate hepcidin expression *in vivo*, but addition of holo-Tf and FAC in the medium suppressed the expression of hepcidin-25. These results conflict with those of some *in vivo* investigations, but other transcriptional studies showed similar data to ours. Reasons for these discordances are still unknown.

Of interest, FAC increased hepcidin-22 expression by an unknown mechanism. DFO suppressed hepcidin-25 expression as expected change, but hepcidin-22 expression was increased. To investigate the effects of bacterial infections, LPS was added to media, and it significantly increased both hepcidin-22 and -25. Hypoxia is also reported to decrease hepcidin expressions [25], while in our studies $CoCl_2$ increased expression of both hepcidin-22 and -25. The furin inhibitor decreased hepcidin-25, but surprisingly hepcidin-22 was increased.

We then determined whether the inclusion of FBS influenced expressions of hepcidin types. Expressions of hepcidin-22 and -25 increased as higher concentrations of FBS were provided in the culture media, an effect that may have been due to the presence of cytokines in the FBS. HepG2 cells were then studied with various stimulants in FBS-free media. As shown in Fig. 5B, hepcidin expression levels were all lower than those determined in FBS-containing medium, and were almost at the limit of measurement by our method, but IL-6 upregulated hepcidin-25 expression. Holo-Tf and FAC depressed both hepcidin-22 and -25, as did the furin inhibitor. The finding that inclusion of FBS significantly influenced the expression of hepcidin deserves consideration from *in vitro* research using cultured cells.

4 Discussion

First developed for assaying prohepcidin [17], studies have used ELISA for measuring hepcidin in serum and urine. Lack of information about the physiological properties and importance of prohepcidin in clinical samples makes interpretation of these studies difficult. The main active isoform of hepcidin is believed to be hepcidin-25, but little information is available about how much translated prohepcidin in hepatocytes is released intact. In fact, Valore and Ganz have pointed out recently that most hepcidin released from the cells is the mature 25-residue form produced by furin [13]. Most recently, Ganz *et al.* developed a novel ELISA system for human serum hepcidin and it is expected that this method will be a powerful tool for clinical investigations, but it is unclear whether this method can be applied for *in vitro* research [23].

Methods utilizing MS-based modalities such as SELDI-TOF-MS have been widely used for measuring hepcidin in serum and urine samples [19]. However, the reliability of SELDI-TOF-MS for quantifying multiple molecules such as hepcidin isoforms is still unclear.

We recently developed a method utilizing LC/ESI-MS/MS for quantification of hepcidin [22]. We aimed to improve and extend this method to apply it for measurement of